

PROGRESS REPORT (1/1/05-31/5/09)

Introduction

Our Achieva 7T MR system, the first ultra-high field system to be supplied by Philips, was installed during this programme: the magnet arrived in autumn 2004 allowing us to commence safety studies which have contributed to national and international safety standards; the console arrived in late summer 2005 allowing 7T scanning to commence; and the multinuclear (^{13}C) channel was delivered at the end of 2008, ^{13}C spectroscopy studies are now underway.

The anticipated improvement in NMR sensitivity at 7T was quickly exploited in implementing very high resolution structural (Fig. 1) and functional MRI. Contrary to the predictions of others, soft tissue contrast was found to be excellent, encouraging us to place increased emphasis on structural imaging in our programme. We anticipated a large gain in BOLD sensitivity but were concerned that this might be limited by physiological noise and image quality issues. In practice we have found that high quality single shot EPI (Fig. 1) can routinely be acquired with robust BOLD signal changes even at high spatial resolution. This has allowed us to achieve one of our programme goals: single trial fMRI. We are now gaining even greater benefits at 7T by further addressing the challenges that are raised by static and radiofrequency field inhomogeneity. Progress against our original objectives is reported below (using the section headings of the original proposal).

Hardware Developments and Effects of Magnetic and RF Field Inhomogeneity

Gradient and Shim Coil Design Our aim is to produce insert gradient and shim coils which improve the performance of the 7 T scanner.

We developed the mathematical formalism needed to design gradient coils on a hemispherical surface [29] and showed that significant performance gains could be achieved by adding a cylindrical extension to the hemisphere, yielding gradient efficiency at fixed inductance that is nearly three times higher than a typical asymmetric, cylindrical head insert coil [151]. A coil set based on this mixed geometry was designed and constructed, and tested at 3 T in experiments using gradient strengths of 100 mTm^{-1} [115] (Fig. 2).

Work on mounting this coil in the 7T scanner is in progress. In parallel with this work, we developed a boundary element method (BEM) [39-41, 54] for designing gradient and shim coils on generally-shaped surfaces. Using this approach we were able to design actively-shielded dome coils [54] with even better performance and a shoulder-slotted gradient and shim coil set (up to 2nd order, with high efficiency, < 100 μH inductance), which was constructed and tested at 3 T [124]. In collaboration with Magnex/Varian we used our versatile BEM software to design "split" gradient coils for a combined PET-MR system [90] and radiotherapy-MR systems. The coil design software is now being used by Varian under licence.

B_0 -Homogeneity A robust image-based procedure, which allows shimming to be focused on targeted brain regions has been implemented at 7 T [91]. First order dynamic shim up-dating has been implemented and shown to produce marginal additional benefits. We also showed that a parcellated dynamic shimming procedure in which the imaging volume is divided up into compact cuboidal volumes for acquisition rather than multiple slices, provides significant improvement in net field homogeneity [55].

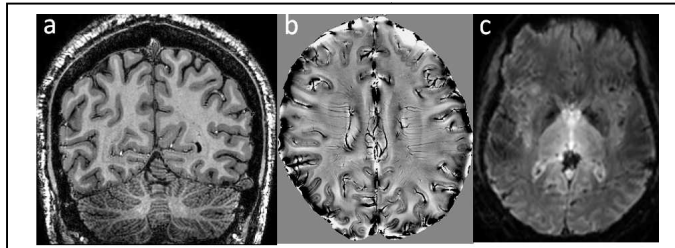


Figure 1 Image quality at 7T: (a) 0.6 mm isotropic resolution MPRAGE (b) 2D gradient echo acquisition ($0.25 \times 0.25 \times 1.5 \text{ mm}^3$) post contrast agent (c) single shot EPI of basal ganglia (1.5 mm, TE = 22 ms). (Ctrl+Click to go to larger version on our website).

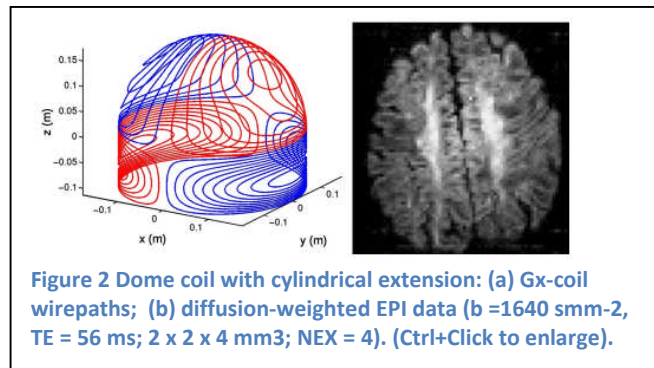


Figure 2 Dome coil with cylindrical extension: (a) Gx-coil wirepaths; (b) diffusion-weighted EPI data ($b = 1640 \text{ smm}^{-2}$, TE = 56 ms; $2 \times 2 \times 4 \text{ mm}^3$; NEX = 4). (Ctrl+Click to enlarge).

RF Hardware and B_1 -Homogeneity Numerical and analytic modelling of 300 MHz coils has demonstrated that no single geometrical structure can generate planar uniform B_1 [68, 71]. Multi-transmit (Multi-Tx) sequences are able to control both homogeneity and SAR. Even though the currently available 7 T hardware does not allow Multi-Tx, we were able to demonstrate a sequential/parallel hybrid system capable of removing RF phase cancellations [116, 117, 120]. This led to further development, modelling and understanding of multiple transmit coil structures [111-113, 118, 119]. A hemispherical eight-element transceiver coil has recently been constructed and tested [114]. A novel double-sided strip-line transceiver surface coil was built, producing reduced local SAR due to the large conservative electric fields being constrained within the dielectric of the probe [112].

High Spatial Resolution

Functional We have optimised strategies for high spatial and temporal resolution fMRI [19, 70], multiecho [26] and outer volume suppression. We have characterised the BOLD response to a simple motor paradigm, as a function of echo time and field strength (1.5, 3 and 7 T) in gradient echo [14] and spin echo [60] experiments. We exploited the increased GE BOLD contrast-to-noise ratio (CNR) to study the

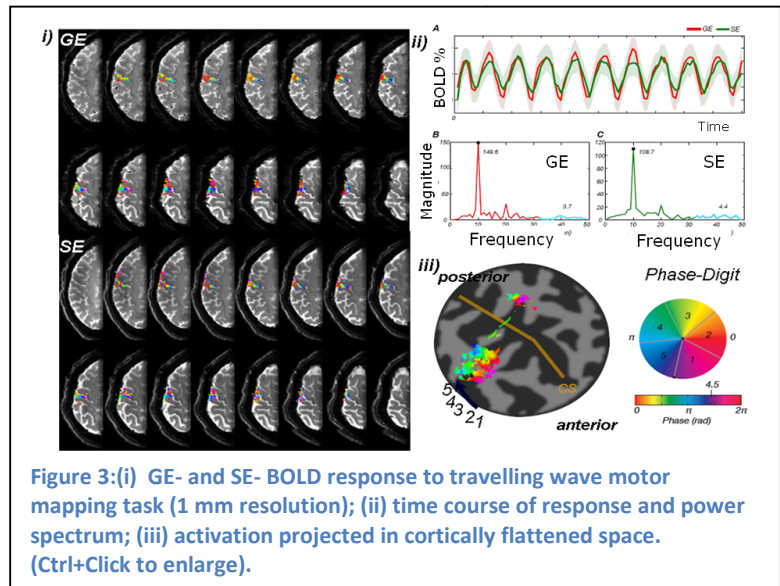


Figure 3:(i) GE- and SE- BOLD response to travelling wave motor mapping task (1 mm resolution); (ii) time course of response and power spectrum; (iii) activation projected in cortically flattened space. (Ctrl+Click to enlarge).

topographic representation of digits in the somatosensory cortex at 1 mm resolution [128], a higher resolution than previously reported in this area. Using a 'travelling wave' paradigm, as has been widely applied in retinotopic mapping [152, 153] we have formed phase maps showing an orderly representation of the digits on the posterior bank of the postcentral gyrus. Event-related paradigms have also been used to characterise the temporal and spatial properties of the haemodynamic response [126]. In these studies we routinely apply threshold-free cluster enhancement [154] and overlay activation maps on inversion recovery-EPI images and high resolution T_2^* -weighted images, to classify tissue type and identify large veins. Image-based shimming [55] reduces residual geometric distortions between EPI and MPRAGE images to less than one voxel, allowing the accurate projection of activation maps onto cortically flattened surfaces. In recent work we further optimised SE-EPI acquisition, improving the fat suppression and refocusing pulse profile to allow contiguous slice acquisition. We are currently completing a study assessing the spatial specificity of SE and GE BOLD contrast in the motor cortex (Fig. 3). We have used fMRI adaptation paradigms and assessed multi-variate pattern classification analysis in the visual cortex at 3T [58], and are now applying these methods at 7T. Using retinotopic mapping at 7T we studied the correspondence of functionally defined V1 and MT to underlying structural anatomy [127] in collaboration with Bridge (Oxford). The optimal contrast for detecting the stria of Gennari at 7T has been assessed by comparing MPRAGE, IR-TSE [125], high resolution 3D GE images; T_2^* -weighted imaging was found to provide best CNR.

Anatomical 7T delivers much better anatomical imaging than initially anticipated; we routinely acquire T_1 - and T_2^* -weighted 3D data at 0.5mm isotropic resolution in 10 minutes, using inversion pulses tailored to operate in the inhomogeneous B_1 fields found at 7T [84]. We have optimized techniques for measuring T_1 which demonstrated good dispersion in T_1 between brain tissues [73] and we developed a novel, contrast based approach to image segmentation [53, 89]. We found an approximately linear variation in R_2^* with field strength [51] and we have developed a number of methods for measuring T_2 [146], including the GESSE sequence which has low sensitivity to RF inhomogeneity [80]. We have

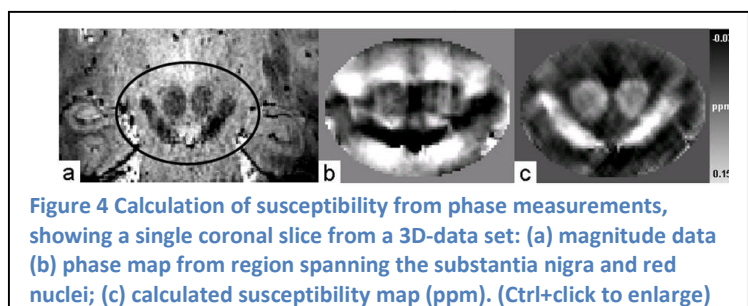


Figure 4 Calculation of susceptibility from phase measurements, showing a single coronal slice from a 3D-data set: (a) magnitude data (b) phase map from region spanning the substantia nigra and red nuclei; (c) calculated susceptibility map (ppm). (Ctrl+click to enlarge)

developed a novel method for acquiring magnetization transfer data, including CEST (chemical exchange saturation transfer) information within the 7T SAR limits. This has allowed us to produce the highest resolution MT brain scans yet reported. We found that the CEST peak due

to chemical exchange with amides is much more pronounced at 7T than 3T [69, 84, 87]. Susceptibility is a particularly important source of contrast at 7T. The phase of gradient echo signals shows the effect of small differences in the magnetic susceptibility. After high-pass filtering, the resulting phase maps show anatomical detail with better CNR than corresponding magnitude images [59, 60, 155]. Such phase variation is also used to enhance the contrast of magnitude images in susceptibility weighted imaging (SWI) [156]. We have pioneered attempts to understand and exploit phase contrast at 7T. We developed a rapid, Fourier-method for calculating the NMR frequency perturbation produced by a general distribution of magnetic susceptibility ($\chi \ll 1$) [42, 43]. This method, which has been used by many other investigators, allows us to simulate phase maps from the human brain [59]. The results show that variations in magnetic susceptibility do cause phase variations that agree with experimental data, but the effects are non local and so care must be taken in interpreting phase maps and SWI data. This problem can be overcome by inverting the simple Fourier domain relationship between frequency and susceptibility [140]. This approach allows quantitative susceptibility maps to be calculated from phase maps [129, 140, 157, 158] and has been validated on phantoms and applied in the human brain (Fig. 4). A simpler fitting process to calculate χ -values can be used if the sample can be described by a small number of homogeneous compartments and we have used this approach to measure in vivo contrast agent (CA) concentration in the human brain after bolus administration [141]. CA has also been used to show that the grey matter/white matter contrast observed in phase and SWI data is not explained by blood volume differences [123]. We have developed methods for scanning post mortem whole brains, dissected brain stems, and brain slices using a dedicated RF coil (Fig. 5). These methods will be used to investigate the relationship between MR images and histology.

Single Trial fMRI, Data Analysis and Physiological Noise

Using parallel imaging and localised image-based shimming methods signal drop out and distortion have not been as problematic as predicted, and the increased CNR at 7T has allowed detection of single trial responses [105, 143]. Initially, we identified a low-level signal instability which compromised single trial studies and was later detected on all Philips 7T scanners; we determined its cause, and proposed a modification to the radiofrequency electronics to resolve it. Philips has adopted our solution and will retrofit it to all its 7T systems. We determined the optimal TR assessing trial-by-trial variations in the amplitude and latency of response [142] and used this to study adaptation to a repeated motor task delivered at variable inter-stimulus intervals [143]. We used concurrent EEG/fMRI at 3T to demonstrate a significant positive correlation between P300 amplitude, BOLD signal and target-to-target interval delay [107], and we used EMG-guided analysis to improve detection of motor responses [16]. We developed a Paradigm Free Mapping technique (PFM) to detect single trial responses with no prior information about the timing of the event [78] and refined this method by using the Danzig selector [104]. This method has been used to detect 'spontaneous events' [122, 159]. We have developed statistical power maps to quantify the effect of variations in spatial sensitivity to BOLD

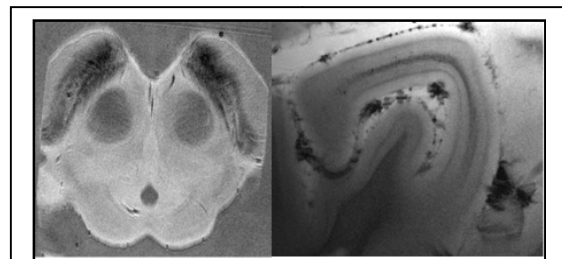


Figure 5 PM images of the substantia nigra (excised brain stem) and Stria of Gennari (whole brain), 0.1 x 0.1 x 0.5 mm3. (Ctrl+click to enlarge).

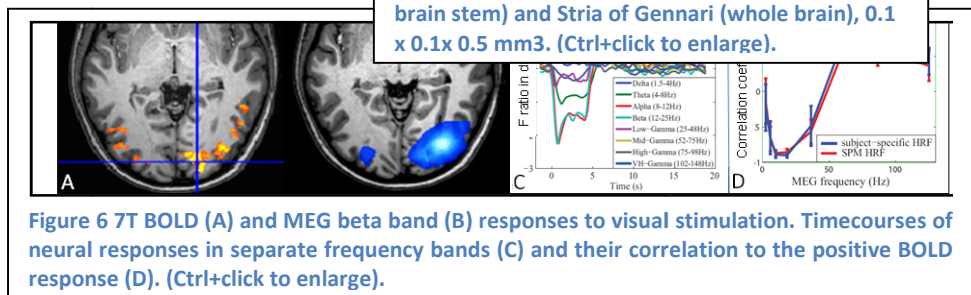


Figure 6 7T BOLD (A) and MEG beta band (B) responses to visual stimulation. Timecourses of neural responses in separate frequency bands (C) and their correlation to the positive BOLD response (D). (Ctrl+click to enlarge).

contrast due to variations in baseline R_2^* and signal at 7T [106], and also investigated the effect of physiological noise on phase data [52].

Quantitative Measures of Brain Activity

EEG/MEG Using data from a 275 channel VSM MEG system (£1.2M SRIF), installed in 2007, we have optimised experiments for our GLM-Beamformer Method [8], extended its use to moving sources, demonstrating MEG retinotopic mapping for the first time [7] and shown how to deal with coherent sources [6]. These methods have demonstrated co-localisation of neural oscillations and fMRI BOLD in visual [3, 132, 133] [77], motor and somatosensory [134] cortices. Strong positive and negative correlations, are observed across a wide range of frequencies [97] (Fig. 6), reproducing previous multiunit activity and field potential results [160]. We have investigated beta band (14-30 Hz) desynchronisation (ERD) during activation

and subsequent synchronisation (ERS) following activation [93], which is thought to be disrupted in Parkinson's and other neurodegenerative diseases. We have developed paradigms in which ERD & ERS are sustained and thus can be examined independently using fMRI [95]. We have demonstrated simultaneous EEG/fMRI studies are possible at 7T [45], and assessed the effect of the EEG system on MR image quality [46]. We showed that suppression of gradient artefacts in the EEG recordings is improved by synchronizing EEG and MR system clocks, and that vectorcardiograms can be used to reduce pulse artefacts [47]. Studies of the origin [75] and field dependence [13] of the pulse artefact, and calculations of the distribution of gradient artefacts over EEG leads [74] should improve this further. Beamformer techniques can be used to suppress residual artefacts [5, 7] and this approach is likely to be adopted by the EEG system manufacturer Brain Products.

Haemodynamic measures/ Modelling the Response to Neuronal Activation We have implemented and optimized pulsed arterial spin labelling (ASL) to measure perfusion (CBF) and arterial blood volume (CBVa) at 7T [18] and shown that background-suppressed ASL [161] significantly reduces physiological noise [139]. We trade the increased perfusion SNR for spatial resolution [110], routinely acquiring data at $1 \times 1 \times 3 \text{ mm}^3$; significantly reducing partial volume errors in the measured perfusion rate. For functional studies, we have developed a double acquisition background suppressed (DABS) scheme [139] providing simultaneous ASL and BOLD measurements. We developed Look-Locker FAIR (LL-FAIR) which provides increased sensitivity to CBF [17], and high sensitivity to CBVa [108] and used this technique to measure single-trial CBF/CBVa changes at 3 T [138]. We are currently investigating the spatial localisation of CBF/CBVa changes to BOLD at 7T [108]. We purchased a RespirAct system that provides independent control of end tidal CO_2 and O_2 , and used this to implement a novel protocol for monitoring the BOLD response to hypercapnia which allows the dynamic relationship between ΔR_2^* and PCO_2 to be studied [81]. We used sinusoidally modulated hypercapnia to obtain the relative timing of the BOLD response [99] and studied the effect of hypercapnia on MEG signals [102]. We proposed a method of using hyperoxia to measure the venous CBV changes [101]. We found that hyperoxia causes field inhomogeneity in the brain and are developing methods to correct for this [100]. We produced a modified model of the dynamic relationship between BOLD signal, CBF, CBV and blood oxygenation that accounts for CBVa changes, and validated it with a contrast agent (CA) experiment [76]. As part of this work we characterized and modelled the relaxivity blood dependence on deoxyhaemoglobin and CA [2], and investigated the echo time dependence of blood T_2 [109]. We optimized contrast enhanced angiograph to obtain 0.3 mm isotropic resolution in peripheral vessels [86].
Neurospectroscopy Improved spectral dispersion at 7T enables reliable quantification of brain glutamate and glutamine using ^1H MRS [44, 121, 131], and this has been exploited in a collaborative study with Stagg (Oxford) to demonstrate the differential polarity effects of direct current stimulation (DCS) on these brain metabolites [61]. A $^1\text{H}/^{13}\text{C}$ coil has recently been delivered for use at 7T and it is being evaluated in ^1H decoupled ^{13}C studies of glycogen repletion following exercise, prior to ^{13}C neurospectroscopy studies.

Applications of 7T

Sensorimotor Function We investigated sensorimotor processing [20, 48, 63] and transformations associated with the planning and control of guided actions [33, 50]. We explored the role of the medial superior parietal lobe in maintaining an up-to-date estimate of limb posture [79]. We also investigated the neural mechanisms underlying planning and control of ocular movements at 3T [64, 162, 163] and 7T [49, 65]. We developed novel MR-compatible devices [32], including pneumatic robot arms to deliver time-varying forces, and pneumatic somatosensory stimulators, for studies of motor prediction and motor learning.

Schizophrenia Combined EEG/fMRI has been used to study the role of EEG oscillations in the recruitment of large scale attentional networks in patients with schizophrenia at 3T [36, 37]. We demonstrated that patients have diminished frontocentral theta EEG activity during an N-back working memory task and diminished BOLD signal in a distributed attentional network that includes insula and frontal regions [38]. This work has led to a MRC grant to study low frequency oscillations in schizophrenia patients at 3 and 7T. We studied lateralization and focalization of somatosensory processing in schizophrenia at 3T [72]; results support the theory that generalised loss of functional specialisation is fundamental to schizophrenia.

High-Resolution Mapping of Functional Sub-Fields in Human Auditory Cortex We were the first to co-localise responses to sound frequency and pitch in humans using fMRI [30], and our subsequent work investigated whether this was a pitch-specific field [31]. In collaboration with Dechent and Voit (Göttingen, Germany), we conducted high-spatial resolution fMRI studies at 3T to assess the cortical location and specificity of frequency, complex pitch, and lateralisation [35, 130]. We recently investigated frequency-specific effects of attentional modulation [88]. Studies of the auditory cortex are particularly challenging due to scanner noise, signal loss and distortion, and extensive cortical folding. We sourced 7T compatible earphones (Sensimetrics

Corporation, Boston, USA) and adapted these to deliver high quality sound. We have now begun a high resolution fMRI study of auditory processing and tonotopicity at 7T.

Multiple Sclerosis We have found [66] that using susceptibility weighted imaging at 7T allows both small parenchymal veins and white matter MS lesions to be identified in a single image set without CA. We have shown that white matter lesions are highly likely (>80%) to be perivenous, whereas ischaemic white matter lesions, are less likely (<20%) to be [137] (Fig. 7). Distinguishing between different types of white matter lesions is a major challenge for clinical diagnosis in MS [164] so potentially our observations will have significant clinical impact. We have demonstrated that 0.5 mm isotropic, MPRAGE at 7T allows the identification and classification of cortical lesions [94]. To date we have scanned 62 subjects. Comparison with DIR sequences at 3T [165] has revealed that many of the apparent lesions detected at 3T are in fact 'false positives' and can be attributed to small blood vessels on the cortical surface [136].

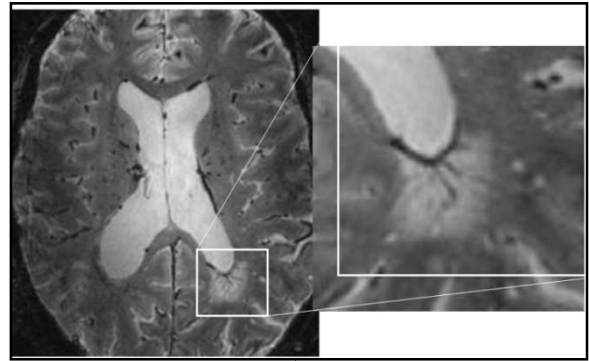


Figure 7 T2* weighted image (0.67mm³ voxels) showing the relationship between vessels and lesions. (Ctrl+click to enlarge).

Interaction of Magnetic Fields with the Human Body

We have an ongoing interest in MR safety [15, 25, 27, 28, 135], but were prompted to give more attention to this work by the European Union Physical Agents EMF Directive (2004) [34]. We established thresholds for transient sensory perceptions (magnetophosphenes, vertigo and metallic taste) in magnetic fields [9, 21], and showed that induced electric fields were the primary mechanism for the sensation of vertigo [21]. We participated in a study of the effect of magnetic fields on cognitive performance and visual acuity [10-12]; this showed a possible weak effect on visual acuity, but no changes were found in visual evoked potentials recorded under switched fields [22]. We performed the first measurements of electric fields induced in the body by changing magnetic fields in MRI [23, 24]; the approach we developed will be used to verify the results of numerical modelling [1] under a recently-awarded EPSRC grant. We also developed a boundary element method for calculating electric fields induced in the human body by changing magnetic fields [57]. The International Commission on Non-Ionizing Radiation issued new guidelines reducing static magnetic field exposure limits [166], citing our recent work.

References

1. Bencsik, M., et al., *Physics In Medicine And Biology*, 2007, 52, 2337-2353.
2. Blockley, N.P., et al., *Magnetic Resonance In Medicine*, 2008, 60, 1313-1320.
3. Brookes, M.J., et al., *Neuroimage*, 2005, 26, 302-308.
4. Brookes, M.J., et al., *Magnetic Resonance In Medicine*, 2007, 58, 41-54.
5. Brookes, M.J., et al., *Neuroimage*, 2008, 40, 1090-1104.
6. Brookes, M.J., et al., *Neuroimage*, 2007, 34, 1454-1465.
7. Brookes, M.J., et al., *Neuroimage*, 2009, 45, 440-452.
8. Brookes, M.J., et al., *Neuroimage*, 2008, 39, 1788-1802.
9. Cavin, I.D., et al., *Journal Of Magnetic Resonance Imaging*, 2007, 26, 1357-1361.
10. de Vocht, F., et al., *Journal Of Magnetic Resonance Imaging*, 2007, 26, 1255-1260.
11. de Vocht, F., et al., *British Journal Of Radiology*, 2007, 80, 822-828.
12. de Vocht, F., et al., *Bioelectromagnetics*, 2007, 28, 247-255.
13. Debener, S., et al., *International Journal Of Psychophysiology*, 2008, 67, 189-199.
14. der Zwaag, W.V., et al., *Neuroimage*, 2009.
15. Dobson, J., et al., *PLOS*, 2009.
16. Francis, S., et al., *Neuroimage*, 2009, 44, 469-479.
17. Francis, S.T., et al., *Magnetic Resonance In Medicine*, 2008, 59, 316-325.
18. Gardener, A.G., et al., *Magn Reson Med*, 2009, 61, 874-82.
19. Gibson, A., et al., *Magnetic Resonance Imaging*, 2006, 24, 433-442.
20. Gibson, A.M., et al., *Solid State Nuclear Magnetic Resonance*, 2005, 28, 258-265.
21. Glover, P.M., et al., *Bioelectromagnetics*, 2007, 28, 349-361.
22. Glover, P.M., et al., *Journal Of Magnetic Resonance Imaging*, 2007, 26, 1353-1356.
23. Glover, P.M., et al., *Physics In Medicine And Biology*, 2007, 52, 5119-5130.
24. Glover, P.M., et al., *Physics In Medicine And Biology*, 2008, 53, 361-373.
25. Gowland, P.A., *Progress In Biophysics & Molecular Biology*, 2005, 87, 175-183.

26. Gowland, P.A., et al., *Physics In Medicine And Biology*, 2007, 52, 1801-1813.
27. Gowland, P.A., et al., *Physics In Medicine And Biology*, 2008, 53, L15-L18.
28. Gowland, P.A., et al., *Journal Of Magnetic Resonance Imaging*, 2007, 26, 1177-1178.
29. Green, D., et al., *Magnetic Resonance In Medicine*, 2005, 54, 656-668.
30. Hall, D.A., et al., *Eur J Neurosci*, 2006, 24, 3601-10.
31. Hall, D.A., et al., *Cereb Cortex*, 2009, 19, 576-85.
32. Jackson, C.P.T., et al., *Neuroimage*, 2008, 40, 1731-1737.
33. Jackson, S.R., et al., *Neuropsychologia*, 2009, 47, 1397-1408.
34. Keevil, S.F., et al., *British Journal Of Radiology*, 2005, 78, 973-975.
35. Krumbholz, K., et al., *Journal Of Neurophysiology*, 2007, 97, 1649-1655
36. Laurens, K.R., et al., *Schizophr Res*, 2005, 75, 159-71
37. Liddle, P.F., et al., *Psychol Med*, 2006, 36, 1097-108.
38. Mallikarjun, P.K., et al., *Schizophrenia Research*, 2008, 98, 199.
39. Marin, L., et al., *Cmes-Computer Modeling In Engineering & Sciences*, 2008, 23, 149-173.
40. Marin, L., et al., *Engineering Analysis With Boundary Elements*, 2008, 32, 658-675.
41. Marin, L., et al., *Boundary Elements and Other Mesh Reduction Methods XXIX*, 2007, 44, 323-332.
42. Marques, J.P., et al., *Concepts In Magnetic Resonance Part B-Magnetic Resonance Engineering*, 2005, 25B, 65-78.
43. Marques, J.P., et al., *Nmr In Biomedicine*, 2008, 21, 553-565.
44. Morris, P., *Journal Of Psychophysiology*, 2006, 20, 328-329.
45. Mullinger, K., et al., *Magnetic Resonance Imaging*, 2008, 26, 968-977.
46. Mullinger, K., et al., *International Journal Of Psychophysiology*, 2008, 67, 178-188.
47. Mullinger, K.J., et al., *Journal Of Magnetic Resonance Imaging*, 2008, 27, 607-616.
48. Newton, J.M., et al., *Neuroimage*, 2005, 24, 1080-1087.
49. Parton, A., et al., *Neuropsychologia*, 2007, 45, 997-1008.
50. Pellijeff, A., et al., *Neuropsychologia*, 2006, 44, 2685-2690.
51. Peters, A.M., et al., *Magnetic Resonance Imaging*, 2007, 25, 748-753.
52. Petridou, N., et al., *Magnetic Resonance Imaging*, 2009, In press.
53. Pitiot, A., et al., *Medical Image Computing and Computer-Assisted Intervention - MICCAI 2007, Pt 1, Proceedings*, 2007, 4791, 759-766.
54. Poole, M., et al., *Concepts In Magnetic Resonance Part B-Magnetic Resonance Engineering*, 2007, 31B, 162-175.
55. Poole, M., et al., *Magnetic Resonance Materials In Physics Biology And Medicine*, 2008, 21, 31-40.
56. Richardson, J.C., et al., *Advanced Drug Delivery Reviews*, 2005, 57, 1191-1209.
57. Sanchez, C.C., et al., *Journal of Engineering Analysis with Boundary Elements*, 2009, 33, 1074-1088.
58. Sapountzis, P., et al., *Perception*, 2008, 37, 164-164.
59. Schaefer, A., et al., *Neuroimage*, 2009, In press.
60. Schaefer, A., et al., *Magnetic Resonance Materials In Physics Biology And Medicine*, 2008, 21, 113-120.
61. Stagg, C., et al., *Journal of Neuroscience*, 2009, In press.
62. Stevenson, E., et al., *International Journal Of Obesity*, 2008, 32, S75-S75.
63. Summers, I.R., et al., *Journal Of The Acoustical Society Of America*, 2009, 125, 1033-1039.
64. Sumner, P., et al., *Perception*, 2007, 36, 170-170.
65. Sumner, P., et al., *Neuron*, 2007, 54, 697-711.
66. Tallantyre, E.C., et al., *Neurology*, 2008, 70, 2076-2078.
67. Tallantyre, E.C., et al., *Investigative Radiology* (in press), 2009.
68. Thomas, D.W.P., et al., *International Journal Of Applied Electromagnetics And Mechanics*, 2007, 26, 183-189.
69. Tyler, D.J., et al., *Magnetic Resonance In Medicine*, 2005, 53, 103-109.
70. van der Zwaag, W., et al., *Magnetic Resonance In Medicine*, 2006, 56, 1320-1327.
71. Vukovic, A., et al., *Ieee Transactions On Medical Imaging*, 2008, 27, 766-774.
72. White, T.P., et al., *Psychiatry Research*, 2009, In press.
73. Wright, P.J., et al., *Magnetic Resonance Materials In Physics Biology And Medicine*, 2008, 21, 121-130.
74. Yan, W.X., et al., *Neuroimage*, 2009, 46, 459-71.
75. Yan, W.X., et al., *Human Brain Mapping*, 2009, 46, 459-71.
76. Blockley, N.P., et al., *Neuroimage*, 2009, Under review.

77. Brookes, M.J., et al., *Neuroimage* 2009, Submitted.
78. Caballero Gaudes, C., et al., *Neuroimage*, 2009, Submitted.
79. Condon, L., et al., *Exp Brain Res*, 2009, In Press
80. Cox, E.F., et al., *Magn Reson Med*, 2009, Submitted.
81. Driver, I., et al., *Magnetic Resonance In Medicine*, 2009, Submitted.
82. Eldeghaidy, S., et al., *Hum Brain Mapp*, 2009.
83. Hall, E., et al., *Magnetic Resonance Medicine*, 2009, Submitted.
84. Hurley, A.C., et al., *Magnetic Resonance in Medicine*, 2009, Submitted.
85. Leggett, J., et al., *Magnetic Resonance in Medicine*, 2009, submitted.
86. Ludman, C.N., et al., *Journal of Magnetic Resonance Imaging*, 2009, Submitted.
87. Mougin, O.M., et al., *Neuroimage*, 2009, Under review.
88. Paltogou, A.E., et al., *Hearing Research*, 2009, Under revision.
89. Pitiot, A., et al., *Neuroimage*, 2009, Submitted.
90. Poole, M., et al., *Magnetic Resonance in Medicine*, 2009, Under revision.
91. Sanchez, R., et al., Submitted to *Neuroimage*, 2009.
92. Sapountzis, P., et al., *Neuroimage*, 2009, submitted.
93. Stevenson, C.M., et al., *Human Brain Mapping*, 2009, Submitted
94. Tallantyre, E.C., et al., *Multiple Sclerosis*, 2009, Submitted.
95. Wang, F., et al. in *Human Brain Mapping*. 2009.
96. Wharton, S., et al., *Neuroimage*, 2009, submitted.
97. Zumer, J.M., et al., submitted to *NeuroImage* 2009.
98. Zumer, J.M., et al., *Human Brain Mapping*, 2009, Submitted.
99. Blockley, N.B., et al. in *17th Annual Meeting of the ISMRM*. 2009.
100. Blockley, N.B., et al. in *17th Annual Meeting of the ISMRM*. 2009.
101. Blockley, N.B., et al. in *26th Annual Scientific Meeting ESMRMB*. 2009.
102. Blockley, N.B., et al., in *Biomagnetism. Interdisciplinary research and exploration*, R. Kakigi, et al., Editors. 2008, Hokkaido University Press.
103. Brookes, M.J., Stevenson, C. M., Hadgipapas, A., Barnes, G. R., Mullinger, K., Bagshaw, A. P., Bowtell, R., Morris, P. G., Vrba, J., in *Biomagnetism. Interdisciplinary research and exploration*, K.Y. R. Kakigi, S. Kuriki, Editor. 2008, Hokkaido University Press.
104. Caballero, C., et al. in *Human Brain Mapping* 2009.
105. Caballero, C., et al. in *17th Annual Meeting of the ISMRM*. 2008.
106. Caballero, C., et al. in *Human Brain Mapping*. 2009.
107. Eldeghaidy, S., et al. in *15th Annual Meeting of the ISMRM*. 2007.
108. Francis, S.T., et al. in *17th Annual Meeting of the ISMRM*. 2009.
109. Gardener, A.G., et al. in *17th Annual Meeting of the ISMRM*. 2009.
110. Hall, E., et al. in *17th Annual Meeting of ISMRM*. 2009.
111. Jones, A., et al. in *ISMRM Workshop on Advances in High-Field MR* 2007.
112. Jones, A., et al. in *15th ISMRM*. 2007.
113. Jones, A., et al. in *14th ISMRM*. 2009.
114. Lee, D., et al. in *17th ISMRM*. 2009.
115. Leggett, J., et al. in *14th Annual Meeting of the ISMRM*. 2006.
116. Magill, A., et al. in *ESMRMB*. 2004.
117. Magill, A., et al. in *16th ISMRM*. 2006.
118. Magill, A., et al. in *ISMRM Workshop on Advances in High-Field MR* 2007.
119. Magill, A., et al. in *ISMRM Workshop on Advances in High-Field MR* 2007.
120. Magill, A., et al. in *13th ISMRM*. 2005.
121. Panek, R., et al. in *16th Annual Meeting of the ISMRM*. 2009.
122. Petridou, N., et al. in *17th Annual Meeting of the ISMRM*. 2009.
123. Petridou, N., et al. in *17th Annual Meeting of the ISMRM*. 2009.
124. Poole, M., et al. in *16th Annual Meeting of the ISMRM*. 2008.
125. Sanchez, R., et al. in *15th Annual Meeting of the ISMRM*. 2007.
126. Sanchez, R., et al. in *17th Annual Meeting of the ISMRM*. 2009.
127. Sanchez, R., et al. in *16th Annual Meeting of the ISMRM*. 2008.
128. Sanchez, R., et al. in *16th Annual Meeting of the ISMRM*. 2008.
129. Schaefer, A., et al. in *16th Annual Meeting of the ISMRM*. 2008.
130. Schönwiesner, M., et al. in *Hum Brain Mapp 13th Meeting*. 2007.

131. Stephenson, M.C., et al. in *17th Annual Meeting of the ISMRM*. 2009.
132. Stevenson, C., et al. in *17th Annual Meeting of the ISMRM*. 2009.
133. Stevenson, C., et al. in *17th Annual Meeting of the ISMRM*. 2009.
134. Stevenson, C., et al., in *Boimagnetism. Interdisciplinary research and exploration*, R. Kakigi, et al., Editors. 2007, Hokkaido University Press. p. 325-328
135. Strydom, M.L., et al., 2005 IEEE/ACES International Conference on Wireless Communications and Applied Computational Electromagnetics, 2005, 389-392.
136. Tallantyre, E., et al. in *17th Annual Meeting of the ISMRM*. 2009.
137. Tallantyre, E., et al. in *17th Annual Meeting of the ISMRM*. 2009.
138. Wesolowski, R., et al. in *15th Annual Meeting of the ISMRM*. 2007.
139. Wesolowski, R., et al. in *17th Annual Meeting of the ISMRM*. 2009.
140. Wharton, S., et al. in *17th Annual Meeting of the ISMRM*. 2009.
141. Wharton, S., et al. in *17th Annual Meeting of the ISMRM*. 2009.
142. Wright, P.J., et al. in *16th Annual Meeting of the ISMRM*. 2008.
143. Wright, P.J., et al. in *16th Annual Meeting of the ISMRM*. 2008.
144. Bowtell, R., *Nature*, 2008, 453, 993-994.
145. Glover, P., et al., *Nature*, 2009, 457, 971-972.
146. Hoad, C.L., et al., *Magnetic Resonance in Medicine*, 2009, Under review.
147. Hoad, C.L., et al., *Journal Of Magnetic Resonance Imaging*, 2006, 24, 1350-1356.
148. Gardener, A.G., et al., *Magnetic Resonance in Medicine*, 2009, Under review.
149. Marques, J.P., et al., *Journal Of Chemical Physics*, 2005, 123.
150. Faber, C., et al., *Journal Of Magnetic Resonance*, 2006, 182, 315-324.
151. Alsop, D.C., et al., *Magnetic Resonance In Medicine*, 1996, 35, 875-886.
152. Engel, S.A., et al., *Cereb Cortex*, 1997, 7, 181-92.
153. Engel, S.A., et al., *Nature*, 1994, 369, 525.
154. Smith, S.M., et al., *Neuroimage*, 2009, 44, 83-98.
155. Duyn, J.H., et al., *PNAS*, 2007, 104, 11796-11801.
156. Haacke, E.M., et al., *Magnetic Resonance Imaging*, 2005, 23, 1-25.
157. Shmueli, K., et al. in *16th Annual Meeting of the ISMRM*. 2008.
158. Liu, T., et al., *MRM*, 2009, 61, 196-204.
159. Fox, M.D., et al., *Nat Rev Neurosci*, 2007, 8, 700-11.
160. Mukamel, R., et al., *Science*, 2005, 309, 951-954.
161. Garcia, D.M., et al., *MRM*, 2005, 54, 366-72.
162. Ryan, S., et al., *Experimental Brain Research*, 2006, 173, 389-394.
163. Smith, D.T., et al., *Neuropsychologia*, 2005, 43, 1288-1296.
164. Miller, A., et al., *J Neurol Sci*, 2008, 274, 68-75.
165. Geurts, J.J., et al., *Radiology*, 2005, 236, 254-60.
166. Ziegelberger, G., *Health Physics*, 2009, 96, 504-514.
167. Preston, T.J., et al., *J Neurosci*, 2008, 28, 11315-27.